Far East Journal of Mathematical Sciences (FJMS)

Published Online: February 2014
Available online at http://pphmj.com/journals/fjms.htm
Volume 84, Number 1, 2014, Pages 123-138

ENTRAINMENT OF SURROUNDING AIR EFFECTS ON THE STABILITY OF PASSIVE CLOUDS CONTAINING WATER DROPLETS

N. R. Djue, Y. Kramoh, E. Danho* and B. D. Asseke

Laboratory of Mechanics
College of Mathematics and Computer Sciences
University FHB of Abidjan-Cocody
22 BP 582 Abidjan 22, Ivory Coast
e-mail: danhoemile@yahoo.com

Abstract

In a previous work, we investigated the stability of passive cloud flows at the stage of condensation and found that this process favored the instability of the flow. In the present paper, we diagnose the capacity of both gravity and entrainment to generate also instability mechanisms in passive cloud flows. The study shows that gravity waves cannot generate instability in the flow, whereas the entrainment is very destabilizing. Moreover, the amplification rate of the unstable modes is proportional to the entrainment rate and the flow becomes more and more unstable along with higher entrainment rate.

I. Introduction

Instabilities mechanisms are common physical phenomena occurring in one phase or multiphase fluid flows (Charru [1], Drazin [2], Danho [5], Takeuchi et al. [11], Timoshin and Smith [9], Malick and Singh [10], de

Received: November 27, 2013; Accepted: January 6, 2014
2010 Mathematics Subject Classification: 86A10.
Keywords and phrases: stability, dispersion relation, clouds, mixing ratio, entrainment rate.
*Corresponding author

Verdière and Te Raa [12], Paşa [13], Wang et al. [14], Zhen et al. [15], Seo [16] and Milleta et al. [20]).

Cloud flows in natural environment display multitude of regimes with variability in space as well as in time. However, any changing in the flow regime is most of the time accompanied by thermodynamics and momentum parameters variation leading to also phase changing in the cloud. All these processes determine the cloud status. The passive clouds are those which do not contain falling droplets and the active ones are those in which raindrops are present. Among many factors that influence the cloud dynamics, instabilities are some of the main mechanisms that impulse the changing. Many works have been done on this matter. Stability of atmospheric clouds flows has intensively been performed these last thirty years along with computational capacities. Most of those studies had been focused on frontal systems instabilities and particularly on conditional symmetric instabilities (Lemaître et al. [24] and Xu and Clark [21-23]). More recently, interest on the study of atmospheric clouds and those involving droplets dynamics as well has increased (Djué et al. [3, 6] and Shima et al. [17], Tao and Moncrieff [18] and Van Weverberg et al. [19]). Focus on interactions between air proper dynamics on the one hand and the cloud formation and maturity towards rainfalls dynamics has also increased (Djué et al. [3, 6], Grabowski et al. [25], Shima et al. [17] and Tao and Moncrieff [18]). On the other hand, these processes are very often sustained by instabilities mechanisms (Djué et al. [6, 8]). Recently, Djue et al. [4] have pointed out that the instability of a convective passive cloud is governed by an entrainment process between the cloud and its surrounding environment and that feeds the cloud parcel. They also found that convective passive clouds are stable to internal and gravity waves in the low atmosphere on the Jean vertical extent scale. In a newer paper, they pointed out [7] that the condensation process also enhances the flow instability in passive clouds.

The present study is conducted to see if the accounting of cloud droplets in the passive cell contain can change the flow instability mechanisms. Indeed in [4], only the water vapor was considered in the cloud composition and this question was raised.

II. Linear Stability of an Isolated Passive Cloud Cell Flow in a Uniform Gravity Field

The model governing the flow is similar to the one used in [3, 7] with a supplementary term accounting for gravity:

$$\begin{cases} \partial_t \rho_a + u\partial_z \rho_a + \rho_a \partial_z u = \xi_1, \\ \partial_t r_1 + u\partial_z r_1 = \xi_2, \\ \partial_t r_2 + u\partial_z r_2 = \xi_3, \\ \partial_t u + u\partial_z u + \dfrac{1}{\rho_a(1+r_1)}\partial_z \rho = \xi_4, \\ \partial_t p + \rho_a(1+r_1)c_s^2 \partial_z u + u\partial_z p = \xi_5, \end{cases} \tag{1}$$

$$\xi_1 = \xi_2 = \xi_3 = \xi_5 = 0 \quad \text{and} \quad \xi_4 = -g(1 + r_1 + r_2). \tag{2}$$

ρ_a, r_1, r_2, u and p are, respectively, the dry air density, the water vapor mixing ratio, the cloud water mixing ratio, the velocity and the pressure, c_s is the sound speed.

It is easy to check that the following hydrostatic equilibrium flow

$$\rho_a^b = \rho_{a_0} = cste; \quad r_1^b = r_{10} = cste; \quad r_2^b = r_{20} = cste; \quad u^b = 0;$$

$$p^b = p_0 - g\rho_{a_0}(1 + r_{10} + r_{20})z; \quad p_0 = cste \tag{3}$$

is a solution of (1).

As usual, we add a perturbation to the above equilibrium stationary flow to investigate its stability. We can write

$$\rho_a = \rho_{a_0} + \tilde{\rho}_a; \quad r_1 = r_{10} + \tilde{r}_1; \quad r_2 = r_{20} + \tilde{r}_2; \quad u = \tilde{u};$$

$$p = (p_0 - g\rho_{a_0}(1 + r_{10} + r_{20})z) + \tilde{p}, \tag{4}$$

so that (1) becomes after linearization

$$\begin{cases} \partial_t \widetilde{\rho}_a + \rho_{a_0} \partial_z \widetilde{u} = 0, \\ \partial_t \widetilde{r}_1 = 0, \\ \partial_t \widetilde{r}_2 = 0, \\ \partial_t \widetilde{u} + \dfrac{g}{\rho_{a_0}} \left(1 + \dfrac{r_{20}}{1 + r_{10}}\right) \widetilde{\rho}_a + \dfrac{g}{1 + r_{10}} \widetilde{r}_1 + \dfrac{g}{1 + r_{10}} \widetilde{r}_2 + \dfrac{1}{\rho_{a_0}(1 + r_{10})} \partial_z \widetilde{p} = 0, \\ \partial_t \widetilde{p} + 1.4(1 - 0.1 r_{10})(p_0 - g\rho_{a_0}(1 + r_{10} + r_{20})z)\partial_z \widetilde{u} \\ \qquad\qquad - g\rho_{a_0}(1 + r_{10} + r_{20})\widetilde{u} = 0. \end{cases} \tag{5}$$

The passive warm cloud model we are dealing with here is applicable to small cumuli at initial formation or fog which are located at altitude not higher than 1500 meters. These altitudes are compatible with the Jean's scale z_h [1, 4],

$$z_h = \frac{1}{(1 - 0.1 r_{10} + r_{20})} \frac{c_0^2}{g} \tag{6}$$

such that

$$\beta_b = 1.4(1 - 0.1 r_{10})(P_0 - g\rho_{a_0}(1 + r_{10} + r_{20})z) \tag{7}$$

can be approximated by

$$\beta_0 = 1.4 P_0 (1 - 0.1 r_{10}). \tag{8}$$

z_h is approximately 9 kms and (5) becomes

$$\begin{cases} \partial_t \widetilde{\rho}_a + \rho_{a_0} \partial_z \widetilde{u} = 0, \\ \partial_t \widetilde{r}_1 = 0, \\ \partial_t \widetilde{r}_2 = 0, \\ \partial_t \widetilde{u} + \dfrac{g}{\rho_{a_0}} \left(1 + \dfrac{r_{20}}{1 + r_{10}}\right) \widetilde{\rho}_a + \dfrac{g}{1 + r_{10}} \widetilde{r}_1 + \dfrac{g}{1 + r_{10}} \widetilde{r}_2 + \dfrac{1}{\rho_{a_0}(1 + r_{10})} \partial_z \widetilde{p} = 0, \\ \partial_t \widetilde{p} + \beta_0 \partial_z \widetilde{u} - g\rho_{a_0}(1 + r_{10} + r_{20})\widetilde{u} = 0. \end{cases} \tag{9}$$

(9) admits solutions in the form $\tilde{x}(z, t) = \hat{x} \exp j(kz - \omega t)$, where $j^2 = -1$. k is the wave number and ω is the pulsation. $k \in \mathbb{R}$ and $\omega \in \mathbb{C}$. We have then to solve the following algebraic system of equations:

$$\begin{cases} -\omega\hat{\rho}_a + k\rho_{a_0}\hat{u} = 0, \\ -\omega\hat{r}_1 = 0, \\ -\omega\hat{r}_2 = 0, \\ -j\omega\hat{u} + \dfrac{g}{\rho_{a_0}}(1 + r_{20})\hat{\rho}_a + \dfrac{g}{1 + r_{10}}\hat{r}_1 + \dfrac{g}{1 + r_{10}}\hat{r}_2 + \dfrac{jk}{\rho_{a_0}(1 + r_{10})}\hat{p} = 0, \\ -\omega\hat{p} + [jk\beta_0 + jg\rho_{a_0}(1 + r_{10} + r_{20})]\hat{u} = 0 \end{cases} \tag{10}$$

which associated dispersion relation is

$$-j\omega^3[\omega^2 - k^2c_0^2] = 0. \tag{11}$$

This leads to

$$\omega_1 = 0, \quad \omega_2 = kc_0 \text{ and } \omega_3 = -kc_0. \tag{12}$$

These neutral modes, already encountered when we studied isolated convective atmospheric cells in a gravity field [4], show us that gravity has no destabilizing effect on passive clouds flow in absence of entrainment.

III. Linear Stability of an Open Passive Cloud Flowing in a Uniform Gravity Field

As the cloud is open, it has exchanges with its surrounding [3, 4]. Let us now account for the entrainment rate in the model governing the cloud flow to investigate the entrainment impact on the flow stability. This model has already been used in [3]. For the present study, the terms present in the equations have been finely computed and the linearization of mixing ratios terms has been done with judicious care. This leads to

$$\begin{cases} \partial_t \rho_a + u\partial_z \rho_a + \rho_a \partial_z u = \xi_1, \\ \partial_t r_1 + u\partial_z r_1 = \xi_2, \\ \partial_t r_2 + u\partial_z r_2 = \xi_3, \\ \partial_t u + u\partial_z u + \dfrac{1}{\rho_a(1+r_1)}\partial_z p = \xi_4, \\ \partial_t p + 1.4p(1-0.1r_1)\partial_z u + u\partial_z p = \xi_5, \end{cases} \tag{13}$$

where

$$\xi_1 = \frac{\gamma\rho_a}{1+r_e}(1+r_1+r_2); \quad \xi_2 = \gamma\left(\frac{r_e}{1+r_e} - r_1\right); \quad \xi_3 = -\gamma r_2;$$

$$\xi_4 = -g(1+r_1+r_2);$$

$$\xi_5 = \gamma\tau_1^e p + \gamma\tau_3^e\rho_a + \gamma\tau_2^e\rho_a r_1 + \gamma\tau_3^e\rho_a r_2 + \gamma\tau_4^e p r_1 + \gamma\tau_5^e p r_2, \tag{14}$$

with

$$\tau_1^e = -\frac{2r_e}{1+r_e} + \frac{1}{2.5}\left(\frac{3.5}{1+r_e} - \alpha_1^e\right); \quad \tau_2^e = 0.2645 C_{p_e}\theta_e;$$

$$\tau_3^e = \frac{C_{p_e}\theta_e}{2.5}; \quad \tau_4^e = \left(\frac{3.103 r_e}{1+r_e} - 2\right) + \frac{1}{2.5}\left(\frac{3.161}{1+r_e} + 2.27\alpha_1^e\right);$$

$$\tau_5^e = \frac{1}{2.5}\left(\frac{3.5}{1+r_e} - \alpha_1^e\right); \quad \alpha_1^e = \frac{C_{p_e}}{R_a}. \tag{15}$$

In the above equations, « e » is relative to the environment.

As the entrainment rate is low, we can see that the equilibrium stationary flow defined in (3) is also solution of (13).

By introducing (4) into (13) and after linearization, we get

$$\begin{cases} \partial_t \widetilde{\rho}_a + \rho_{a_0} \partial_z \widetilde{u} - \dfrac{\gamma}{1+r_e} \rho_{a_0} \widetilde{r}_1 - \dfrac{\gamma}{1+r_e}(1+r_0)\widetilde{\rho}_a = 0, \\ \partial_t \widetilde{r}_1 + \gamma \widetilde{r}_1 = 0, \\ \partial_t \widetilde{r}_2 + \gamma \widetilde{r}_2 = 0, \\ \partial_t \widetilde{u} + \dfrac{g(1+r_{20})}{\rho_{a_0}} \widetilde{\rho}_a + \dfrac{g}{1+r_{10}} \widetilde{r}_1 + \dfrac{g}{1+r_{10}} \widetilde{r}_2 + \alpha_0 \partial_z \widetilde{p} = 0, \\ \partial_t \widetilde{p} + \beta_b \partial_z \widetilde{u} - g\eta^0 \widetilde{u} - \gamma(\tau_1^e + \tau_4^e r_{10} + \tau_5^e r_{20})\widetilde{p} \\ \qquad - \gamma(\tau_3^e(1+r_{20}) + \tau_2^e r_{10})\widetilde{\rho}_a - \gamma(\tau_4^e p^b + \tau_2^e \rho_{a_0})\widetilde{r}_1 - \gamma \tau_4^e p^b \widetilde{r}_2 = 0, \end{cases} \tag{16}$$

$$\eta^0 = 1 + r_{10} + r_{20}, \qquad \alpha_0 = \frac{1}{\rho_{a0}(1+r_{10})}. \tag{17}$$

Working again within the Jean's scale z_h range $(z \ll z_h)$, the approximations lead to a homogeneous system of PDEs which modal solutions verify the following system:

$$\begin{cases} (\gamma \pi_{10} - j\omega)\hat{\rho}_a + jk\rho_{a_0}\hat{u} + \gamma \pi_{20}\hat{r}_1 + \gamma \pi_{20}\hat{r}_2 = 0, \\ (-j\omega + \gamma)\hat{r}_1 = 0, \\ (-j\omega + \gamma)\hat{r}_2 = 0, \\ -j\omega\hat{u} + \pi_{30}\hat{\rho}_a + \pi_{40}\hat{r}_1 + \pi_{40}\hat{r}_2 + jk\alpha_0\hat{p} = 0, \\ -(j\omega + \gamma(\tau_1^e + \tau_4^e r_{10} + \tau_5^e r_{20}))\hat{p} + (j\beta_0 k - g\rho_{a_0}\eta^0)\hat{u} \\ \qquad - \gamma(\tau_3^e(1+r_{20}) + \tau_2^e r_{10})\hat{\rho}_a - \gamma(\tau_4^e P_0 + \tau_2^e \rho_{a_0})\hat{r}_1 - \gamma \tau_4^e p_0 \hat{r}_2 = 0, \end{cases} \tag{18}$$

where

$$\pi_{10} = -\frac{1}{1+r_e}(1 + r_{10} + r_{20}); \quad \pi_{20} = -\frac{\rho_{a_0}}{1+r_e};$$

$$\pi_{30} = \frac{g(1+r_{20})}{\rho_{a_0}}; \quad \pi_{40} = \frac{g}{1+r_{10}}. \tag{19}$$

The dispersion relation associated to (18) is

$$(-j\omega+\gamma)^2[(\gamma\pi_{10}-j\omega)[j\omega(j\omega+\gamma(\tau_1^e+\tau_4^e r_{10}+\tau_5^e r_{20}))$$
$$-jk\alpha_0(j\beta_0 k-g\rho_{a_0}\eta^0)]$$
$$-jk\rho_{a_0}[-\pi_{30}(j\omega+\gamma(\tau_1^e+\tau_4^e r_{10}+\tau_5^e r_{20}))$$
$$+jk\alpha_0\gamma(\tau_3^e(1+r_{20})+r_2^e r_{10})]]=0 \quad (20)$$

that gives either

$$(-j\omega+\gamma)^2=0 \Leftrightarrow \omega=-j\gamma \quad (21)$$

or

$$(\gamma\pi_{10}-j\omega)[j\omega(j\omega+\gamma(\tau_1^e+\tau_4^e r_{10}+\tau_5^e r_{20}))-jk\alpha_0(j\beta_0 k-g\rho_{a_0}\eta^0)]$$
$$-jk\rho_{a_0}[-\pi_{30}(j\omega+\gamma(\tau_1^e+\tau_4^e r_{10}+\tau_5^e r_{20}))$$
$$+jk\alpha_0\gamma(\tau_3^e(1+r_{20})+\tau_2^e r_{10})]=0 \quad (22)$$

$$\Leftrightarrow$$

$$j\omega^3-\gamma[\pi_{10}-(\tau_1^e+\tau_4^e r_{10}+\tau_5^e r_{20})]\omega^2$$
$$-j[k^2c_0^2-\gamma^2\pi_{10}(\tau_1^e+\tau_4^e r_{10}+\tau_5^e r_{20})]\omega+\gamma\pi_{10}(k^2c_0^2+jkg\rho_{a_0}\alpha_0\eta^0)$$
$$+jk\pi_{30}\rho_{a_0}\gamma(\tau_1^e+\tau_4^e r_{10}+\tau_5^e r_{20})+k^2\rho_{a_0}\alpha_0\gamma(\tau_3^e(1+r_{20})+\tau_2^e r_{10})=0, \quad (23)$$

since

$$g\rho_{a_0}\eta^0\alpha_0=\rho_{a_0}\pi_{30} \text{ and } \alpha_0\beta_0=c_0^2. \quad (24)$$

Finally, (23) can be rewritten

$$\omega^3+j\gamma[\pi_{10}-(\tau_1^e+\tau_4^e r_{10}+\tau_5^e r_{20})]\omega^2$$
$$-[k^2c_0^2-\gamma^2\pi_{10}(\tau_1^e+\tau_4^e r_{10}+\tau_5^e r_{20})]\omega$$

$$+ k\rho_{a_0}\gamma[\pi_{30}(\tau_1^e + \tau_4^e r_{10} + \tau_5^e r_{20}) + \pi_{10} g\alpha_0\eta^0]$$

$$- jk^2\gamma[\pi_{10}c_0^2 + \rho_{a_0}\alpha_0(\tau_3^e(1 + r_{20}) + \tau_2^e r_{10})] = 0. \quad (25)$$

Let us note that (25) is in the form

$$\omega^3 + a\omega^2 + b\omega + c = 0, \quad (26)$$

where

$$a = j\gamma[\pi_{10} - (\tau_1^e + \tau_4^e r_{10} + \tau_5^e r_{20})], \quad (27)$$

$$b = -[k^2 c_0^2 - \gamma^2\pi_{10}(\tau_1^e + \tau_4^e r_{10} + \tau_5^e r_{20})], \quad (28)$$

$$c = k\rho_{a_0}\gamma[\pi_{30}(\tau_1^e + \tau_4^e r_{10} + \tau_5^e r_{20}) + \pi_{10} g\alpha_0\eta^0]$$

$$- jk^2\gamma[\pi_{10}c_0^2 + \rho_{a_0}\alpha_0(\tau_3^e(1 + r_{20}) + \tau_2^e r_{10})]. \quad (29)$$

The using of Cardan method leads to

$$\omega_1 = \left(\sqrt[3]{\alpha_1} - \frac{l}{\sqrt[3]{\alpha_1}}\right)\cos\left(\frac{\phi}{3}\right)$$

$$+ j\left[\left(\sqrt[3]{\alpha_1} + \frac{l}{\sqrt[3]{\alpha_1}}\right)\sin\left(\frac{\phi}{3}\right) - \frac{1}{3}\gamma[\pi_{10} - (\tau_1^e + \tau_4^e r_{10} + \tau_5^e r_{20})]\right], \quad (30)$$

$$\omega_2 = \left(\sqrt[3]{\alpha_1} - \frac{l}{\sqrt[3]{\alpha_1}}\right)\cos\left(\frac{\phi - 2\pi}{3}\right)$$

$$+ j\left[\left(\sqrt[3]{\alpha_1} + \frac{l}{\sqrt[3]{\alpha_1}}\right)\sin\left(\frac{\phi - 2\pi}{3}\right) - \frac{1}{3}\gamma[\pi_{10} - (\tau_1^e + \tau_4^e r_{10} + \tau_5^e r_{20})]\right], \quad (31)$$

$$\omega_3 = \left(\sqrt[3]{\alpha_1} - \frac{l}{\sqrt[3]{\alpha_1}}\right)\cos\left(\frac{\phi + 2\pi}{3}\right)$$

$$+ j\left[\left(\sqrt[3]{\alpha_1} + \frac{l}{\sqrt[3]{\alpha_1}}\right)\sin\left(\frac{\phi + 2\pi}{3}\right) - \frac{1}{3}\gamma[\pi_{10} - (\tau_1^e + \tau_4^e r_{10} + \tau_5^e r_{20})]\right], \quad (32)$$

where

$$l = \frac{1}{3}\gamma^2[\pi_{10} - (\tau_1^e + \tau_4^e r_{10} + \tau_5^e r_{20})]^2 - k^2 c_0^2, \tag{33}$$

$$\alpha_1^2 = \frac{1}{4}k^2\gamma^2[[\pi_{10} - (\tau_1^e + \tau_4^e r_{10} + \tau_5^e r_{20})]kc_0^2 - g]^2 + \left[\frac{2}{3\sqrt{3}}k^3 c_0^3 + k^2[\pi_{10}c_0^2 + \rho_{a_0}\alpha_0(\tau_3^e(1 + r_{20}) + r_2^e r_{10})\right]^2. \tag{34}$$

Taking each mode alone, it is not easy to determine algebraically the sign of the imaginary part. However, we can see that their sum is a pure imaginary complex number:

$$\omega_1 + \omega_2 + \omega_3 = -j\gamma[\pi_{10} - (\tau_1^e + \tau_4^e r_{10} + \tau_5^e r_{20})]. \tag{35}$$

The computation of $[\pi_{10} - (\tau_1^e + \tau_4^e r_{10} + \tau_5^e r_{20})]$ gives

$$\pi_{10} - (\tau_1^e + \tau_4^e r_{10} + \tau_5^e r_{20}) = -\frac{1 + (1 + 2.44)r_{10} + r_{20}}{1 + r_e} + \frac{4.9r_e}{1 + r_e} + \frac{r_e(2.9r_{20} - 4.54r_e r_{10})}{1 + r_e}. \tag{36}$$

As the mixing ratios are weak (of order 10^{-2}), then $\pi_{10} - (\tau_1^e + \tau_4^e r_{10} + \tau_5^e r_{20})$ is a negative number. Since in general $\gamma > 0$, therefore the imaginary part of the sum $\omega_1 + \omega_2 + \omega_3$ is positive. This means that at least one among the eigen frequencies has a positive imaginary part. This result is sufficient to conclude that the flow is destabilized when the cloud is nourished by its surrounding through the entrainment process in which $\gamma > 0$. Moreover, when the cloud loses mass and energy for the benefit of its surrounding by an entrainment process in which $\gamma < 0$, we remark that the flow is still destabilized since from (21), $\omega = -j\gamma$ has a positive imaginary part. So, whatever the sense of the exchange between the open cloud cell and its surrounding, the entrainment lets the cloud cell unstable. This result is confirmed by the direct simulations. Some results of these simulations are presented below for respectively $\gamma = 10^{-4}$; $\gamma = 10^{-3}$; $\gamma = 10^{-2}$ and $\gamma = 0$:

Case $\gamma = 10^{-4}$**.**

$\omega_1 = -324.5352 + (4.7721e-005)i$
$\omega_2 = 324.5352 + (4.7721e-005)i$
$\omega_3 = 1.4131e-008 - (2.4666e-006)i$

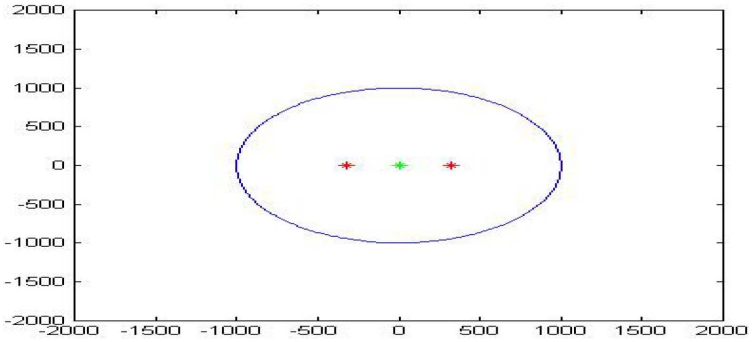

Figure 1. Eigen frequencies for $\gamma = 10^{-4}$.

Case $\gamma = 10^{-3}$**.**

$\omega_1 = -324.5352 + (4.7721e-004)i$
$\omega_2 = 324.5352 + (4.7721e-004)i$
$\omega_3 = 1.4131e-007 - (2.4666e-005)i$

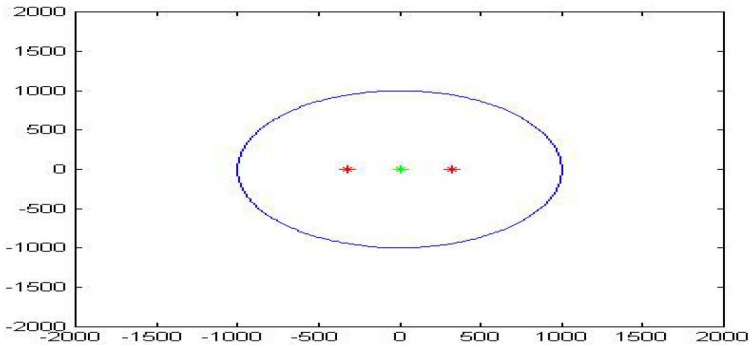

Figure 2. Eigen frequencies for $\gamma = 10^{-3}$.

Case $\gamma = 10^{-2}$**.**

$\omega_1 = -324.5352 + 0.0048i$
$\omega_2 = 324.5352 + 0.0048i$
$\omega_3 = 1.4131e-006-(2.4666e-004)i$

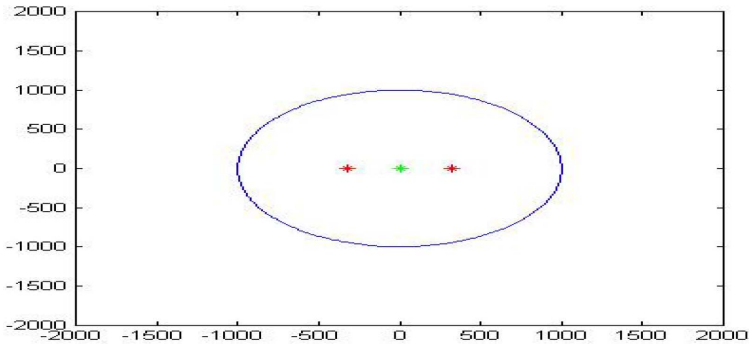

Figure 3. Eigen frequencies for $\gamma = 10^{-2}$.

Case $\gamma = 0$**.**

$\omega_1 = 324.5352$
$\omega_2 = -324.5352$
$\omega_3 = 0$

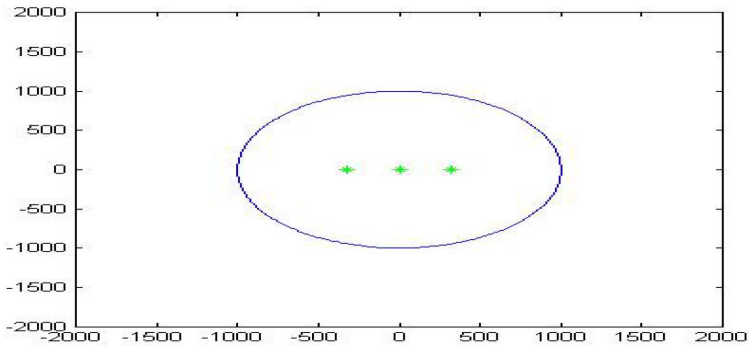

Figure 4. Eigen frequencies for $\gamma = 0$.

Results and comments

The simulations confirm the theoretical results. The red dots on the figures represent unstable modes affixes whereas the green ones represent the stable modes. When $\gamma \neq 0$, there are two unstable modes ω_1 and ω_2, as illustrated by Figure 1, Figure 2 and Figure 3. The stable mode ω_3 is very close to 0. It appears that the real part of the unstable modes ω_1 and ω_2 does not depend on the entrainment rate γ. This real part defines the instability waves speed that is linked to the sound speed c_0. The two unstable modes ω_1 and ω_2 have the same imaginary part that is very dependent upon the entrainment rate γ. We observe that this dependence is linear when we run the model for different values of γ from 0. For the stable mode ω_3, the real part as well as the imaginary part are linearly dependent upon γ. Moreover, the result of the simulation for the case $\gamma = 0$ (Figure 4) shows that $\omega_3 = 0$ as well as the imaginary parts of the modes ω_1 and ω_2. Finally, we must say that the entrainment has a destabilizing effect on the passive cloud flows, in the presence of cloud water.

IV. Conclusion

The present paper aimed to investigate the impact of the surrounding air entrainment rate on the stability of small cumuli and fogs assimilated to passive clouds involving very small droplets flows. Those clouds matured inside the Jean's layer of thickness less than 9 kms from the ground and their stability is not affected by gravity waves. However, any nourishment of these clouds or dissipation of them by an entrainment of the surrounding environment makes them become very unstable to any infinitesimal perturbation. The digital simulations revealed that the instability is strongly governed by the entrainment rate. The entrainment process characterizes roughly the melting of the cloud cell with its nearby environment through an instability mechanism. We showed that the amplification rate of the unstable modes is proportional to the entrainment rate γ. Thus, the higher the value of the entrainment rate, the more unstable the flow becomes and is susceptible

to develop a chaotic behavior. The present result has already been pointed out in [4]. However, in [4], cloud droplets were not taken into account in the model and the question was, if they had been, the results would have been the same? Moreover, in [4], we did not know how the amplification rate varied with the entrainment rate. The present study closes definitely the question: gravity does not destabilize passive clouds flows whereas exchange of the cloud cell with its surrounding through the entrainment process generates an instability mechanism in the flow leading to potential changes in its dynamics as well as thermodynamics.

References

[1] F. Charru, Instabilités Hydrodynamiques, Savoir Actuelle, CNRS Édition, 2007.

[2] P. Drazin, Hydrodynamic Stability, Cambridge University Press, 1991.

[3] R. N. Djué, E. Danho, M. K. Sangaré, B. Coulibaly and K. K. S. Yanga, Model development for the evolution of active warm clouds and analysis of environmental atmospheric hygrometry impact on raindrops production, Adv. Appl. Fluid Mech. 3(1) (2008), 89-103.

[4] N. R. Djue, Y. Kramoh, E. Danho and S. K. K. Yanga, On the stability of convective atmospheric flows, Asian J. Appl. Sci. 6(1) (2013), 29-39.

[5] E. Danho, On some properties of Kelvin-Helmholtz two-phase flows instability modes, Africa Matematika, Série 3, Vol. 10, 1999.

[6] Ndri Roger Djué and Emile Danho, Impact of the atmospheric impulsional instability on the production of raindrops in active warm clouds modeling, African J. Sci. Tech. (AJST) 7(2) (2006), 134-143.

[7] N. R. Djue, Y. Kramoh, E. Danho and D. B. Asseke, Linear stability of passive clouds flows, Far East J. Math. Sci. (FJMS) 84(1) (2014), 65-80.

[8] N. R. Djue, Y. Kramoh, E. Danho and D. B. Asseke, Challenging effects of self-conversion and capture processes on the stability of active clouds flows, Adv. Appl. Fluid Mech. 15(2) (2014), 117-129.

[9] S. N. Timoshin and F. T. Smith, Non-local interactions and feedback instability in a high Reynolds number flow, Theoret. Comput. Fluid Dyn. 17(1) (2003), 1-18

[10] S. K. Malick and M. Singh, Nonlinear Kelvin-Helmholtz instability in hydromagnetics, Astrophysics and Space Sciences 109 (1985), 231-239.

[11] H. Takeuchi, N. Suzuki, K. Kasamatsu, H. Saito and M. Tsubota, Shear-flow instability in two-component Bose-Einstein condensates, J. Low Temp. Phys. 158(3-4) (2010), 384-390.

[12] Alain Colin de Verdière and L. Te Raa, Weak oceanic heat transport as a cause of the instability of glacial climates, Climate Dynamics 35(7-8) (2010), 1237-1256.

[13] Gelu Paşa, Stability analysis of diffusive displacement in three-layer Hele-Shaw cell or porous medium, Trans. Porous Media 85(1) (2010), 317-332.

[14] Zhi-Liang Wang, S. P. Lin and Zhe-Wei Zhou, Spatio-temporal instability of two-layer liquid film at small Reynolds numbers, Appl. Math. Mech. - Engl. Ed. 31(1) (2010), 1-12.

[15] Li Zhen, Hu Guo-Hui and Zhou Zhe-We, Floquet instability of a large density ratio liquid-gas coaxial jet with periodic fluctuation, Appl. Math. Mech. - Engl. Ed. 29(8) (2008), 975-984.

[16] Taewon Seo, A numerical study of the spatial stability of three-dimensional developing plane mixing layer, KSME International J. 11(6) (1997), 696-704.

[17] S. Shima, K. Kusano, A. Kawano, T. Sugiyama and S. Kawahara, The super-droplet method for the numerical simulation of clouds and precipitation: a particle-based and probabilistic microphysics model coupled with a non-hydrostatic model, Quart. J. Roy. Meteor. Soc. 135(642) (2009), 1307-1320.

[18] Wei-Kuo Tao and Mitchell W. Moncrieff, Multiscale cloud system modeling, Reviews of Geophysics 47(4) (2009), RG4002.

[19] Kwinten Van Weverberg, Nicole P. M. van Lipzig and Laurent Delobbe, The impact of size distribution assumptions in a bulk one-moment microphysics scheme on simulated surface precipitation and storm dynamics during a low-topped supercell case in Belgium, Monthly Weather Review 139(4) (2011), 1131-1147.

[20] S. Milleta, F. Rousset, V. Botton and H. Ben Hadid, Stability analysis of stratified coating flow of shear-thinning fluids, Eur. Phys. J. Special Topics 166 (2009), 143-146.

[21] Q. Xu and J. H. E. Clark, The nature of symmetric instability and its similarity to convective and inertial instability, J. Atmos. Sci. 42 (1985), 2880-2883.

[22] Q. Xu, Conditional symmetric instability and mesoscale rainbands, Quart. J. Roy. Meteor. Soc. 112 (1986), 315-334.

[23] Qin Xu, Completeness of normal modes for symmetric perturbations in vertically bounded domain, J. Meteor. Soc. Japan 89(4) (2011), 389-394.

[24] Y. Lemaître, G. Scialom and A. Protat, Conditional symmetric instability, frontogenetic forcing and rain-band organization, Quart. J. Roy. Meteor. Soc. 127(578) (2001), 2599-2634.

[25] Wojciech W. Grabowski, Odile Thouron, Jean-Pierre Pinty and Jean-Louis Brenguier, A hybrid bulk-bin approach to model warm-rain processes, J. Atmos. Sci. 67(2) (2010), 385-399.